PUB-76-169-E
E-0331

E-331

Physical Review Letters 37, 799 (1976)

2

Inclusive μ-Pair Production at 150 GeV by π^+ Mesons and Protons*

K. J. Anderson, G. G. Henry, K. T. McDonald,† J. E. Pilcher,‡

and E. I. Rosenberg

Enrico Fermi Institute, University of Chicago

Chicago, Illinois 60637

and

J. G. Branson, G. H. Sanders, A.J.S. Smith, and J. J. Thaler

Joseph Henry Laboratories, Princeton University,

Princeton, New Jersey 08540

(Submitted to the XVIII Conf. in High-Energy Physics, Tbilisi, USSR, 1976)

ABSTRACT

We report measurements of inclusive μ-pair production by 150 GeV protons and π^+ mesons on beryllium. Absolute cross sections as well as the Feynman-x and P_T dependence are presented in the mass region 0.211 to 3.5 GeV. Upper limits are also given for the inclusive production of η and ρ'(1600) mesons.

We have recently completed a measurement at Fermilab of inclusive μ-pair production by 150 GeV protons and π^+ mesons on beryllium. Results for J production have already been reported.[1] In this paper we report on some of the lower mass resonances and the μ-pair continuum.

The measurements were carried out with the Chicago Cyclotron Spectrometer in Fermilab's Muon Laboratory. The beam, spectrometer, and trigger logic have already been described.[1] For most of the results presented here eight additional planes of multiwire proportional chambers were used. A module of four planes (XYUV) was placed at the upstream face of the hadron shield, centered on the beam 100 cm downstream from the target. A second module of four planes was placed with similar orientation halfway through the shield. The (X,Y) and (U,V) wire planes each formed an orthogonal coordinate system and were oriented at 45° to each other. These detectors improved the effective mass resolution by a factor of 2.5 and provided strong discrimination against μ-pairs arising from secondary interactions in the shield. Using the methods discussed below we determined that the rejection power is greater than 15 at a mass of 300 MeV and rises sharply with increasing μ-pair mass to over 100 at a mass of 1 GeV.

To study the effectiveness of the event reconstruction in the presence of the extra hadron tracks in the upstream detectors, Monte Carlo generated μ-pairs were superimposed on the actual data recorded in these chambers. The standard reconstruction program was used and the reconstruction efficiency measured as a function of Feynman-x (x_F), P_T, and the mass of the pair. At a typical x_F of 0.3, the reconstruction efficiency was independent of μ-pair mass above 500 MeV. It was lower by a factor of 2 at 325 MeV. The kinematic minimum is $2M_\mu$ = 211 MeV.

A similar method was used to determine the rejection power against background from the shield. Monte Carlo generated μ-pairs originating in the first absorption length of the shield, were added to the data of normal events. The reconstruction efficiency for such events was determined and

we obtained the rejection power described above.

Figure 1 shows the $\mu^+\mu^-$ mass spectrum for data with x_F greater than 0.15 after correction for detector acceptance.[2] The measured line width for the ρ-ω signal is 100 MeV. Both the pion and proton induced data have a strong continuum signal at low mass which falls steeply with increasing mass.

In considering possible background sources for the continuum signal there are several important points. First, the muons of the low mass pairs are overwhelmingly of opposite charge. Like-sign pairs occur at the level of one percent, so that any background source must produce correlated muons. Second, the requirement $x_F > 0.15$ provides suppression against low energy background. Third, since the event trigger and data analysis require an interaction in the target, the only background from the shield is through secondary interactions rather than primary beam interactions. We have estimated the magnitude of this secondary production by using only track trajectories seen downstream from the shield and searching for $J \to \mu^+\mu^-$ events originating in the shield. Such events can be clearly identified and occur at 30% of the level of $J \to \mu^+\mu^-$ from the target. Finally because of our upstream analysis, we have an additional rejection power against shield produced background which is greater than 15.

Among the background sources we have considered quantitatively are photon conversion into μ-pairs in the target or shield, ρ-ω production in the shield, and K^+K^- associated production and leptonic decay. All these sources combined can account for no more than 10% of the observed signal. We conclude that the signal is real and discuss below possible sources for the continuum.

To study the dependence of μ-pair production on the longitudinal and transverse momenta of the pair (x_F and P_T), the data were divided into six mass intervals as specified in Table I. Figure 2 compares $Ed\sigma/dx_F$ for μ-pair production by protons and positive pions. In all mass intervals, pions are more effective than protons in producing μ-pairs of large x_F. The x_F dependence is substantially steeper at low masses than at high. The dependence has been fit to the form $(1-x_F)^c$ and the resulting fits are shown in Fig. 2 and recorded in Table I. For the mass regions III and IV, which contain the ρ-ω and φ signals, fits have also been done after a subtraction of the continuum component. Within statistical errors, the shapes are independent of the subtraction. The results for the shapes, specified in Table I and Fig. 2, are those without subtraction.

It should be noted that in order to gain statistics in mass interval VI, which corresponds to J production, the proportional chambers upstream of the shield were not used in the analysis. These detectors were only available for the latter portion of the data taking run.

The P_T dependence of μ-pair production has been studied in a similar way to the x_F dependence. Figure 3 shows the data for proton and π^+ production. The data are fit to the form $d\sigma/dP_T/P_T \propto \exp(-bP_T)$. Because this function is a poor representation of the data at very low P_T we eliminate the first bin from the fit. Within statistical errors there are no significant differences between the proton and pion induced P_T spectra. There is the definite trend however that the mean transverse momentum of the pairs increases with increasing mass. This is as true for the continuum regions as for the vector mesons.

If the Lorentz invariant cross section is parameterized as $Ed^3\sigma/d^3p = A(1-x_F)^c \exp(-bP_T)$, the normalization parameter A is given in

Table I for each of the mass regions. Because a clear signal for ρ-ω production is seen even without the use of the upstream detectors it is possible to check the normalization using only detectors downstream of the shield. The normalizations from the two analyses agree to better than 10%.

Table I gives the integrated cross sections for $x_F > 0.15$. To obtain the total cross section for the whole forward hemisphere three methods have been used: (1) extrapolate the fit of $Ed\sigma/dx_F$ to $x_F = 0$, (2) extrapolate the fit of $d\sigma/dx_F$ to $x_F = 0$, (3) assume that $Ed\sigma/dx_F$ is constant for $x_F < 0.15$. Methods (2) and (3) give total cross section estimates which agree to 10% for all mass intervals. The estimate of method (1) is within this tolerance in the high mass interval but becomes systematically larger as the μ-pair mass decreases reaching a 60% excess in the lowest mass interval. The results of method (2) are presented in Table I and the error associated with the extrapolation is increased in the lower mass intervals.

Production cross sections from a free nucleon target are determined from our measurements with beryllium, using the A dependence obtained by Binkley et al.[3] We use an $A^{0.67}$ variation for $M_{\mu\mu} < 1.13$ GeV, $A^{0.85}$ for $1.13 < M_{\mu\mu} < 2.0$, and A for $M_{\mu\mu} < 2$ Gev.

The data of Table I, together with known branching ratios[4] can be used to deduce the total inclusive production cross sections for the vector mesons. If we take $\sigma_\rho = \sigma_\omega$, as is consistent with the observed line width, we obtain 8.6±2.5 mb for each of ρ and ω production by protons, 660±200 μb for φ production, and 94±31 nb for J production.

For the observed continuum signal there are a number of simple sources which must exist at some level. The branching ratio $\Gamma(\eta \to \mu^+\mu^-\gamma)/\Gamma(\eta \to \gamma\gamma)$

is calculated to be[5] 7.5×10^{-4}. If all the data with $M_{\mu\mu} < 450$ MeV are attributed to this source we obtain an upper limit for inclusive η production by protons of 11 mb/nucleon. This is to be compared with the 8.6 mb/nucleon for ρ production.

The process $\omega \to \pi^0\mu^+\mu^-$ is calculated to have a branching ratio of $\Gamma(\omega \to \pi^0\mu^+\mu^-)/\Gamma(\omega \to \pi^0\gamma)$ of[6] 5.5×10^{-4}. Thus the expected μ-pair signal from this source is approximately 60% of that from $\omega \to \mu^+\mu^-$ or 13% of the low mass continuum using the assumption that $\sigma_\rho = \sigma_\omega$.

An upper limit on the production of the $\rho'(1600)$ and decay to μ-pairs can be based on the data in mass interval V. We obtain an upper limit of $B\sigma < 6$ nb/nucleon from the proton induced data.

We would like to acknowledge the support received from Fermilab and in particular R. Lundy and his staff in the Neutrino Laboratory. We are indebted to the technical support groups at both Chicago and Princeton Universities. One of us (J.E.P.) would like to acknowledge valuable discussions with C. Rubbia during the formative stage of the experiment. The Chicago-Harvard-Illinois-Oxford muon scattering collaboration is responsible for providing much of the apparatus.

REFERENCES

1. K. J. Anderson et al., Phys. Rev. Lett. 36, 237 (1976).

2. The acceptance calculation uses a flat decay angular distribution for the μ-pair. Our analysis of ρ-ω decays gives a distribution of $1-(0.07\pm0.24)\cos^2\theta$. A decay asymmetry at the one standard deviation level would produce a 5% change in the overall acceptance.

3. M. Binkley et al., Dimuon Production in Nuclear Targets, Columbia University preprint (to be published).

4. For ρ and ω decays we assume μ-e universality and use the e^+e^- storage ring data. Thus $\Gamma(\rho \to \mu^+\mu^-)/\Gamma(\rho \to \text{all}) = 4.3 \times 10^{-5}$, $\Gamma(\omega \to \mu^+\mu^-)/\Gamma(\omega \to \text{all}) = 7.6 \times 10^{-5}$. We also use $\Gamma(\phi \to \mu^+\mu^-)/\Gamma(\phi \to \text{all}) = 2.5 \times 10^{-4}$, $\Gamma(J \to \mu^+\mu^-)/\Gamma(J \to \text{all}) = 0.07$.

5. C. Jarlskog and H. Pilkuhn, Nucl. Phys. B1, 264 (1967); and C. Quigg and J. D. Jackson, Lawrence Berkeley Laboratory report UCRL-18487.

6. C. H. Lai and C. Quigg, private communication.

* Research supported by the National Science Foundation and the Energy Research and Development Administration, and performed at the Fermi National Accelerator Laboratory.

† Enrico Fermi Postdoctoral Fellow

‡ Alfred P. Sloan Foundation Fellow

TABLE CAPTION

Table I — Results of fitting the Lorentz invariant cross section to the form $Ed^3\sigma/d^3p = A(1-x_F)^c \exp(-bP_T)$ for different mass regions. The x_F and P_T projections of the data were fit independently. Calculation of the integrated cross sections is described in the text.

FIGURE CAPTIONS

Figure 1a — Muon-pair effective mass. Pion and proton-induced data are combined to show more clearly the resonance line shapes and the proportion of continuum signal. Events are weighted to correct for acceptance.

Figure 1b — Effective mass spectrum for proton induced μ-pairs.

Figure 1c — Effective mass spectrum for pion induced μ-pairs.

Figure 2 — Dependence of μ-pair production on Feynman-x. The lines represent fits of the form $(1-x)^c$. The best-fit parameters are given in Table I.

Figure 3 — Dependence of μ-pair production on transverse momentum. The lines represent fits of the form $d\sigma/dP_T/P_T \propto \exp(-bP_T)$. The lowest P_T bin is excluded from the fit. Best-fit parameters are given in Table I.

Table I

Region	Mass GeV	Source	A $nb/GeV^2/c^3$	b $(GeV/c)^{-1}$	c	Cross Section /Nucleus $x_F > 0.15$ nb	Cross Section/Nucleon $x_F > 0.15$ nb	Cross Section/Nucleon $x_F > 0$ nb
				Proton Production				
I	0.21 - 0.45	Continuum	$2.67\pm.53 \times 10^4$	4.63±.15	6.03±.22	1470±300	340±70	1550±620
II	0.45 - 0.65	Continuum	$9.03\pm1.8 \times 10^3$	4.58±.14	4.34±.21	800±160	185±37	620±220
III	0.65 - 0.93	ρ-ω	$4.69\pm.95 \times 10^3$	3.79±.09	2.79±.12	960±190	220±44	510±150
		Continuum	$1.83\pm.40 \times 10^3$			372±75	86±17	200±60
IV	0.93 - 1.13	φ	$1.06\pm.21 \times 10^3$	3.93±.28	4.06±.40	127±38	29±9	83±25
		Continuum	$.55\pm.11 \times 10^3$			66±20	15±5	43±13
V	1.13 - 2.0	Continuum	250±100	3.41±.85	3.78±.80	39±16	6.0±2.5	16±7
VI	2.7 - 3.5	J	36±12	2.08±.26	2.94±.32	14±5	1.6±.6	3.3±1.1
				Pion Production				
I	0.21 - 0.45	Continuum	$2.20\pm.44 \times 10^4$	5.07±.25	4.30±.33	1660±330	383±76	1250±500
II	0.45 - 0.65	Continuum	$4.02\pm.80 \times 10^3$	4.64±.24	1.92±.25	780±160	180±37	370±130
III	0.65 - 0.93	ρ-ω	$3.41\pm.70 \times 10^3$	4.31±.16	1.34±.14	960±190	220±44	370±110
		Continuum	$1.46\pm.30 \times 10^3$			410±82	94±20	160±50
IV	0.93 - 1.13	φ	$4.90\pm1.5 \times 10^2$	3.61±.40	1.73±.44	160±48	37±11	70±21
		Continuum	$1.47\pm.44 \times 10^2$			48±14	11±3	21±6.4
V	1.13 - 2.0	Continuum	89±53	3.2±2.4	1.33±1.0	40±24	6.2±3.7	10±6
VI	2.7 - 3.5	J	81±27	2.57±.36	1.72±.38	35±12	3.9±1.3	6.5±2.2

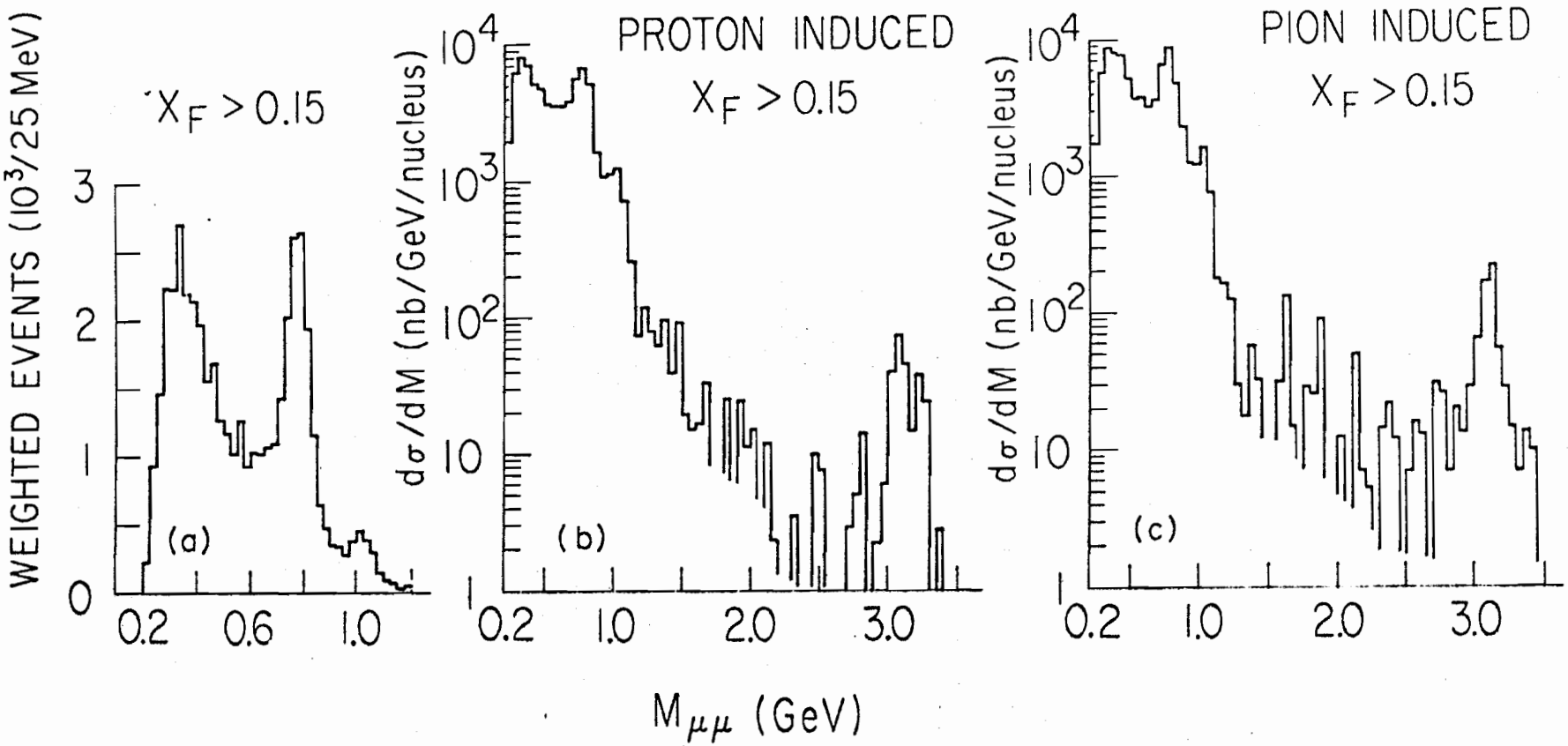
WEIGHTED EVENTS (10^3/25 MeV)
$X_F > 0.15$
(a)
0
1
2
3
0.2
0.6
1.0
$d\sigma/dM$ (nb/GeV/nucleus)
PROTON INDUCED
$X_F > 0.15$
(b)
10^4
10^3
10^2
10
1
0.2
1.0
2.0
3.0
$d\sigma/dM$ (nb/GeV/nucleus)
PION INDUCED
$X_F > 0.15$
(c)
10^4
10^3
10^2
10
1
0.2
1.0
2.0
3.0
$M_{\mu\mu}$ (GeV)

Fig. 1

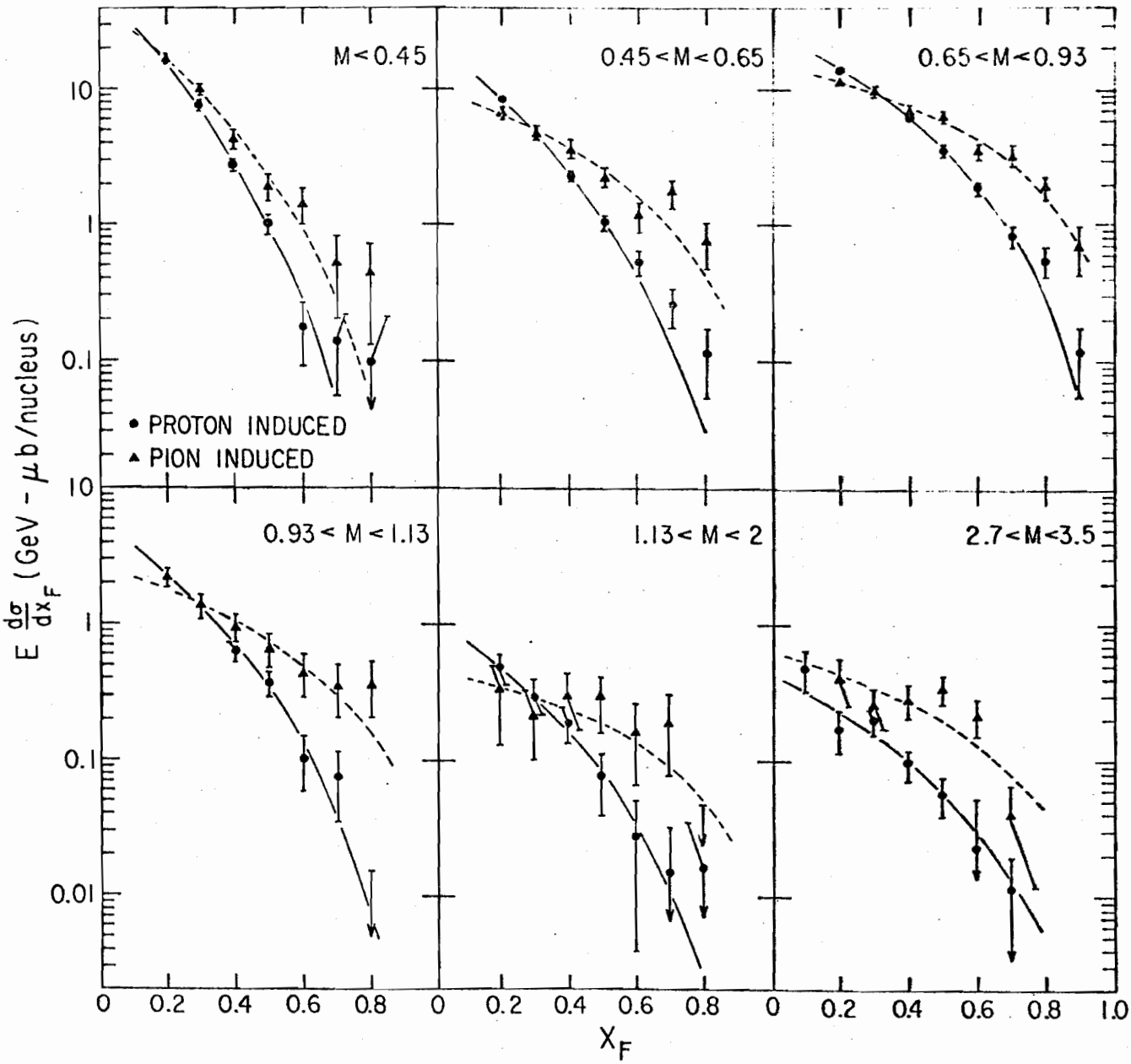
M<0.45
0.45<M<0.65
0.65<M<0.93
0.93<M<1.13
1.13<M<2
2.7<M<3.5
• PROTON INDUCED
▲ PION INDUCED
E dσ/dx_F (GeV - μb/nucleus)
X_F
10
1
0.1
0.01
0
0.2
0.4
0.6
0.8
1.0

Fig. 2

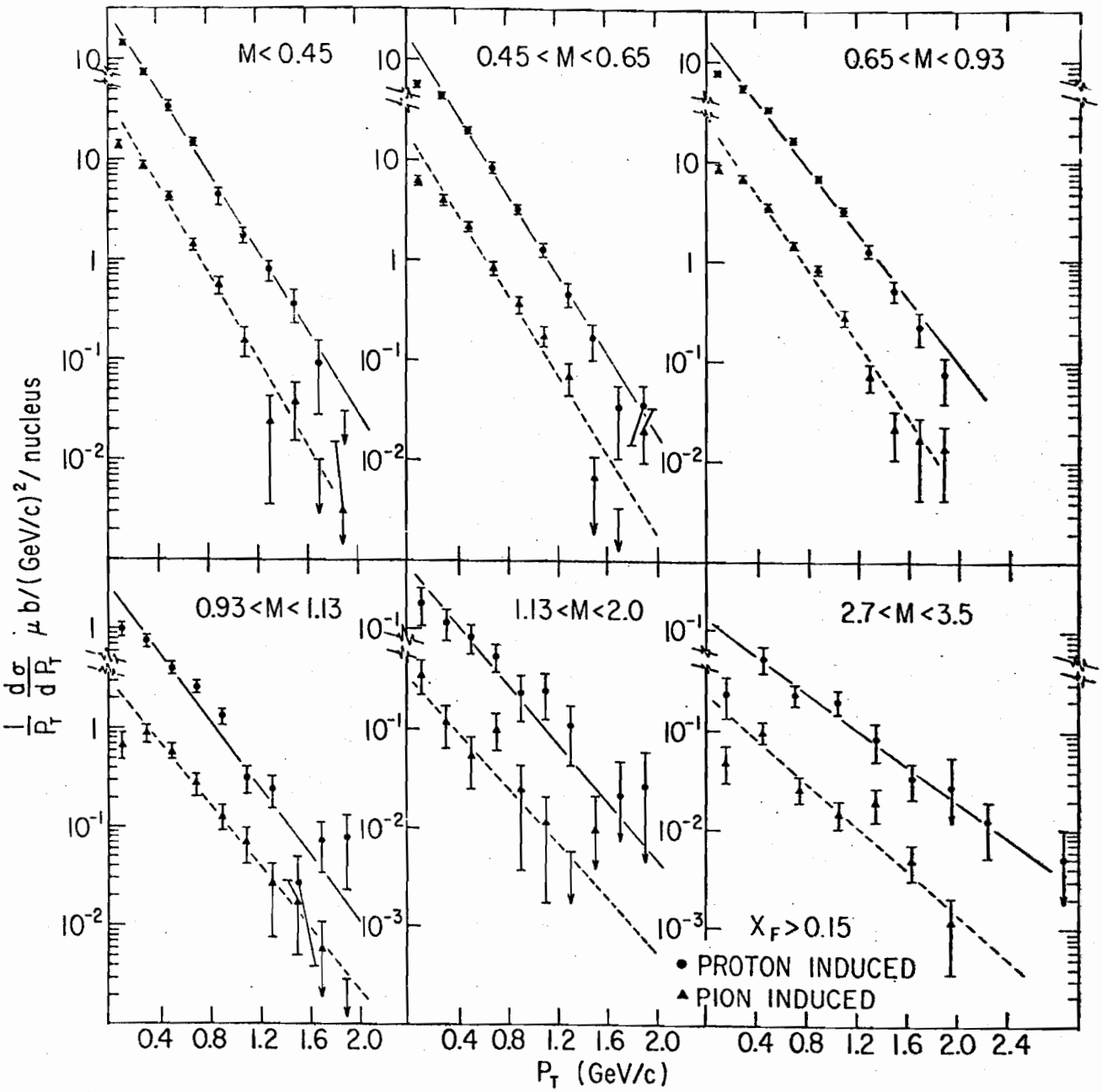
M< 0.45
0.45 < M < 0.65
0.65 < M < 0.93
0.93 < M < 1.13
1.13 < M < 2.0
2.7 < M < 3.5
$X_F > 0.15$
• PROTON INDUCED
▲ PION INDUCED
$\frac{1}{P_T}\frac{d\sigma}{dP_T}$ μb/(GeV/c)²/nucleus
P_T (GeV/c)

Fig. 3